Quantum-electrodynamic calculation of hyperfine-state populations in atomic sodium

P. M. Farrell, W. R. MacGillivray, and M. C. Standage
School of Science, Griffith University, Nathan, Brisbane, Queensland 4111, Australia
(Received 24 December 1987)

A quantum-electrodynamic (QED) description of the resonant interaction of monochromatic light with the $3^2S_{1/2}(F'=2)\rightarrow 3^2P_{3/2}(F=3,2,1)$ hyperfine transitions of the sodium D_2 line is formulated in terms of the Heisenberg atomic operator. Off-diagonal state coherences and all relaxation terms are included. It is found that the equations for the populations, optical coherences, and certain state coherences form a closed subset of the total system of equations. This subset is small enough to be computed numerically. The results of calculations with this model are compared with three previously developed semiclassical descriptions using the density operator. One of the semiclassical models was developed to describe the interaction of weak light with the atomic transition while another is suitable in the case of high-intensity light. For both π and σ excitation it is shown that the QED calculated values for the time-averaged, excited-level population probability converge to those of each of the semiclassical models in the appropriate limit of light intensity. For homogeneous broadening, results show that the optimum light intensity to obtain the largest fraction of atoms in the $3^2P_{3/2}$ level after transversing a 1-mm-diam laser beam is 1.15 mW/mm^2 for π excitation and 1.43 mW/mm^2 for σ excitation.

I. INTRODUCTION

Radiation from lasers and radiation from conventional light sources differ considerably in their degree of coherence, the most coherent light source being a single-mode, continuous-wave laser. When such light interacts resonantly with an atom, the coherence is transferred. Thus the description of the time evolution of such an interaction is quite complex, particularly when the participating atomic energy levels consist of a manifold of degenerate and near-degenerate states, such as in the case of the much-investigated sodium D transitions.

The number of energy states participating in the interaction can be reduced experimentally by, for example, employing a well-collimated atomic beam and optically pumping with the light. If σ^+-polarized radiation is tuned to excite the sodium D_2 line hyperfine transition $3^2S_{1/2}(F'=2)\rightarrow 3^2P_{3/2}(F=3)$, then the atoms can be prepared in the two-state system consisting of the $m_{F'}=2$ ground state and the $m_F=3$ excited state.[1-3] If the sodium atoms interact with linearly polarized light the energy levels cannot be described as simply as for σ excitation. If more than one of the excited-level hyperfine states is excited, coherences will be formed between those of the same m_F values but different F. These coherences are the origin of quantum beats.[4] Their inclusion in a very weak laser-field model used to calculate the frequency-dependent polarization of fluorescence from the D_2 line gives better agreement with experimental results than when they are omitted.[5]

The simplest theoretical approach to describing the excitation of the sodium D_2 transition has been to use rate equations.[6-8] However, these equations do not include coherences other than those implicit in the Einstein coefficients and so fail to depict the coherent nature of the interaction (for example, Rabi nutations), although they do provide a good qualitative picture of the population evolution, particularly at weak radiation intensities.

Semiclassical models which make use of optical Bloch equations have been employed widely to describe atomic and molecular interactions with coherent light.[9] In the vast majority of cases, the models have included only two or three energy states. Recently, McClelland and Kelley[10] have extended this method, with some approximations, to the excitation scheme $3^2S_{1/2}(F'=2)\rightarrow 3^2P_{3/2}(F=3,2)$ in the sodium D_2 line. The time evolution of the populations of the 20 states was calculated for σ^+ polarization. Their overriding reason for performing a more sophisticated population calculation was to allow a more exact interpretation of data from experiments in which electrons are superelastically scattered from sodium target atoms prepared in the $3^2P_{3/2}$ states by single-mode laser light pumping.[11-13]

Most approximations have aimed at reducing the number of coupled differential equations to be solved. To completely describe the interaction of light with a complex atomic system, such as the sodium D_2 transition in hyperfine representation, requires a set of equations numbering of the order of n^2, where n is the number of participating states. By their approximations, McClelland and Kelley reduced the number of equations in their systems from 400 to 38. In the work presented here, we show that, without making any but the usual approximations, the number of equations needed to be solved for particular parameters is much fewer than n^2. This is because the manifold of equations describing the total system contains closed subsets. For example, for π excitation of the $3^2S_{1/2}(F'=2)\rightarrow 3^2P_{3/2}(F)$ hyperfine transitions in sodium, instead of 289, the number of equations required to describe the time evolution of the populations

of the 17 participating states can be reduced, ultimately, to 34.

It is the purpose of this work to use a quantum-electrodynamic (QED) description of the resonant interaction of single-mode, coherent radiation with the homogeneously broadened $3^2S_{1/2}(F'=2)\rightarrow 3^2P_{3/2}(F)$ sodium transitions to calculate the time evolution of the state populations. Even at moderate laser powers, the excitation rate from the $F'=1$ ground state will not be significant in a highly collimated atomic beam and so this channel is treated as a relaxation channel only. All states in the system that can participate are included as well as all nonzero coherences. All relaxation quantities that arise from the derivation are included and it is shown that omission of the generalized relaxation terms leads to some differences in the population calculations.

In Sec. II the QED model is derived and applied to the sodium D_2 transition. Next, the semiclassical model is briefly reviewed, including the McClelland-Kelley version of it. Finally, a recently reported method[14] of simplifying the state description at relatively high laser powers is extended so that comparisons can be made with the other models. In Sec. III the results of calculations of state population probabilities by the theories are presented and discussed, and conclusions are drawn in Sec. IV.

II. THEORY

A. Quantum-electrodynamic theory

We consider, in this section, a full quantum-electrodynamic approach to the description of coherent radiation excitation of an atomic transition. The derivation is in terms of Heisenberg equations of motion of the atomic operator σ, which has matrix elements given by

$$\sigma_{ij}=|i\rangle\langle j| \ . \tag{1}$$

The method follows closely that introduced by Ackerhalt *et al.*[15] and Ackerhalt and Eberly[16] for a two-level atom and extended to a three-level, stepwise scheme by Whitley and Stroud.[17] In the Heisenberg picture, it is also possible to derive an equation of motion for each field mode operator, thus yielding an easily tractable solution to the interaction.

It will be assumed that the injected coherent radiation is tuned to near resonance with an atomic transition which consists of ground- and excited-state manifolds of degenerate and near-degenerate substates. The system Hamiltonian is represented by

$$H=H_A+H_F+H_I \ , \tag{2}$$

where H_A is the free-atom part and can be written as

$$H_A=\sum_m E_m\sigma_{mm} \ , \tag{3}$$

where E_m is the energy of substate $|m\rangle$.

As is usual, the field part is expressed in terms of a_λ and $a_\lambda^\dagger$, the annihilation and creation operators, respectively, for the mode λ, viz.,

$$H_F=\hbar\sum_\lambda \omega_\lambda a_\lambda^\dagger a_\lambda \ . \tag{4}$$

ω_λ is the frequency of the mode. The interaction Hamiltonian H_I can be expressed, in normal ordering, as

$$H_I=\hbar\sum_e\sum_g\sum_\lambda (g_{eg}^\lambda\sigma_{eg}a_\lambda+g_{eg}^{\lambda *}a_\lambda^\dagger\sigma_{ge}) \ , \tag{5}$$

where g_{eg}^λ is the coupling constant taken here as

$$g_{eg}^\lambda=-i\hat{\mathbf{e}}_\lambda\cdot\mathbf{D}_{eg}(2\pi\omega_\lambda/\hbar V)^{1/2} \ , \tag{6}$$

where $\hat{\mathbf{e}}_\lambda$ is the polarization vector of the λ mode and the dipole element is

$$\mathbf{D}_{eg}=\langle e|\mathbf{D}|g\rangle \ . \tag{7}$$

The Heisenberg equation of motion for the field operator a_λ is given by

$$\dot{a}_\lambda=-\frac{i}{\hbar}[a_\lambda,H] \ . \tag{8}$$

Evaluating Eq. (8) yields

$$\dot{a}_\lambda=-i\omega_\lambda a_\lambda-i\sum_e\sum_g g_{eg}^{\lambda *}\sigma_{ge} \ . \tag{9}$$

Formal integration of this equation results in[9]

$$a_\lambda(t)=a_\lambda(0)e^{-i\omega_\lambda t}-i\sum_e\sum_g g_{eg}^{\lambda *}\int_0^t\sigma_{ge}(t')e^{-i\omega_\lambda(t-t')}dt' \ . \tag{10}$$

The operator elements σ_{ge} oscillate with a time scale of the order of the inverse of the transition frequency; thus, for times short compared with the period of the Rabi oscillation or the excited-state lifetime, the atoms can be considered to evolve freely.[9,15–17]

From the operator equation

$$\dot{\sigma}_{ge}=-\frac{i}{\hbar}[\sigma_{ge},H_A] \ , \tag{11}$$

we obtain

$$\sigma_{ge}(t')=\sigma_{ge}(t)e^{i(\omega_e-\omega_g)(t-t')} \ , \tag{12}$$

where ω_e and ω_g are the frequencies of the states $|e\rangle$ and $|g\rangle$, respectively. Substituting Eq. (12) into Eq. (10) then gives for the field,

$$a_\lambda(t)=a_\lambda(0)e^{-i\omega_\lambda t}-i\sum_e\sum_g g_{eg}^{\lambda *}\sigma_{ge}(t)\int_0^t e^{-i(\omega_\lambda-\omega_e+\omega_g)(t-t')}dt' \ . \tag{13}$$

Using the Heisenberg equation of motion for the atomic operator, we now derive an expression for the element representing the optical coherence $\sigma_{e'g'}$. After some working, the equation reduces to

$$\dot{\sigma}_{e'g'}=-i(\omega_{g'}-\omega_{e'})\sigma_{e'g'}-i\sum_e\sum_\lambda g_{eg'}^{\lambda *}a_\lambda^\dagger\sigma_{e'e}+i\sum_g\sum_\lambda g_{e'g}^{\lambda *}a_\lambda^\dagger\sigma_{gg'} \ . \tag{14}$$

Substituting the solution for the field operator, Eq. (13), into Eq. (14) gives, after carrying out appropriate summations,

$$\dot{\sigma}_{e'g'} = -i(\omega_{g'}-\omega_{e'})\sigma_{e'g'} - i\sum_{e}\sum_{\lambda} g_{eg'}^{\lambda *} e^{i\omega_\lambda t} a_\lambda^\dagger(0)\sigma_{e'e} + i\sum_{g}\sum_{\lambda} g_{e'g}^{\lambda *} e^{i\omega_\lambda t} a_\lambda^\dagger(0)\sigma_{gg'} - \sum_{g}\sum_{e''}\sum_{\lambda} g_{e'g}^{\lambda *} g_{e''g}^{\lambda}\sigma_{e''g'}\int_0^t e^{i(\omega_\lambda-\omega_{e''}+\omega_g)(t-t')}dt' \ . \tag{15}$$

It is assumed that the driving field initially consists of a single, coherent mode ω_L. Hence the summation over the modes in the second and third terms of Eq. (15) are replaced by this single value. The integral of the fourth term of this equation has been evaluated and discussed several times previously[9,15,16,18] and gives rise to a damping term (real part) and a frequency shift (imaginary part). For terms of the form

$$\sum_{g}\sum_{\lambda} |g_{e'g}^{\lambda}|^2 \int_0^t e^{i(\omega_\lambda-\omega_{e'}+\omega_g)(t-t')}dt' \ ,$$

the damping terms are proportional to the Einstein A coefficients and the imaginary terms are the usual level Lamb shifts and so can be considered to be incorporated in the definition of the transition frequencies. All other terms arising from the summation over the excited states $|e''\rangle$ lead to generalized damping and shift terms.[19–21]

The generalized damping terms are nonzero when two or more near-degenerate excited states are connected to a common ground state. The generalized shift terms are nonzero only when the nondegenerate excited states have different principal quantum numbers.[21] In this paper we are considering transitions for which this condition does not hold and we accordingly set the generalized shift terms to zero. The real part of the integral is $\pi\delta(\omega_\lambda-\omega_{e'}+\omega_g)$. The generalized decay term involving the ground state $|g\rangle$ is defined as

$$\Gamma_{e'e''g} = \sum_{\lambda}[g_{e'g}^{\lambda *} g_{e''g}^{\lambda}\pi\delta(\omega_\lambda-\omega_{e''}+\omega_g) + g_{e''g}^{\lambda} g_{e'g}^{\lambda *}\pi\delta(\omega_\lambda-\omega_{e'}+\omega_g)] \ . \tag{16a}$$

The decay rate from state $|e'\rangle$ to $|g\rangle$ is given by

$$\Gamma_{e'g} = \Gamma_{e'e'g} \ , \tag{16b}$$

while the total decay rate from an excited state $|e'\rangle$ is

$$\Gamma_{e'} = 2\sum_{g}\sum_{\lambda} |g_{e'g}^{\lambda}|^2 \pi\delta(\omega_\lambda-\omega_{e'}+\omega_g) \ , \tag{16c}$$

where the summation over g includes all states to which $|e'\rangle$ can relax.

Equation (16a) is simplified if the approximation is made that the δ functions take their nonzero values at the same frequency; that is, when $\omega_{e''}-\omega_g$ equals $\omega_{e'}-\omega_g$. Where the two transition frequencies differ by up to the order of rf, the error arising from this approximation will be small since the solution will vary slowly compared with atomic lifetimes. If the two transition frequencies are well separated, then the relaxation terms will oscillate rapidly and can be neglected.

The rapidly oscillating terms in Eq. (15) are removed by applying the standard transformation to the slowly varying operators[17]

$$\chi_{eg} = \sigma_{eg} e^{-i\omega_L t} \ . \tag{17}$$

All other operator elements transform directly. The expectation value of Eq. (15) is then taken. Operator equations of motion for the other atomic operator elements are similarly derived, yielding the general expressions

$$\langle\dot{\chi}_{e'e''}\rangle = -i(\omega_{e''}-\omega_{e'})\langle\chi_{e'e''}\rangle - i\sum_{g}\Omega_{e''g}\langle\chi_{e'g}\rangle + i\sum_{g}\Omega_{e'g}\langle\chi_{ge''}\rangle - \sum_{e}\sum_{g}\sum_{\lambda} g_{e''g}^{\lambda} g_{eg}^{\lambda *}\pi\delta(\omega_\lambda-\omega_e+\omega_g)\langle\chi_{e'e}\rangle - \sum_{e}\sum_{g}\sum_{\lambda} g_{e'g}^{\lambda *} g_{eg}^{\lambda}\pi\delta(\omega_\lambda-\omega_e+\omega_g)\langle\chi_{ee''}\rangle \ , \tag{18a}$$

$$\langle\dot{\chi}_{g'g''}\rangle = -i(\omega_{g''}-\omega_{g'})\langle\chi_{g'g''}\rangle - i\sum_{e}\Omega_{eg''}\langle\chi_{g'e}\rangle + i\sum_{e}\Omega_{eg'}\langle\chi_{eg''}\rangle + \sum_{e'}\sum_{e}\sum_{\lambda} g_{e'g''}^{\lambda *} g_{eg'}^{\lambda}\pi\delta(\omega_\lambda-\omega_e+\omega_{g'})\langle\chi_{ee'}\rangle + \sum_{e'}\sum_{e}\sum_{\lambda} g_{e'g'}^{\lambda *} g_{eg''}^{\lambda}\pi\delta(\omega_\lambda-\omega_e+\omega_{g''})\langle\chi_{e'e}\rangle \ , \tag{18b}$$

$$\langle\dot{\chi}_{e'g'}\rangle = -i\Delta_{e'g'}\langle\chi_{e'g'}\rangle + i\sum_{g}\Omega_{e'g}\langle\chi_{gg'}\rangle - i\sum_{e}\Omega_{eg'}\langle\chi_{e'e}\rangle - \sum_{e}\sum_{g}\sum_{\lambda} g_{e'g}^{\lambda *} g_{eg}^{\lambda}\pi\delta(\omega_\lambda-\omega_e+\omega_g)\langle\chi_{eg'}\rangle \ , \tag{18c}$$

where $\Delta_{e'g'}$ is the detuning between the field and transition frequencies $\omega_{e'g'}$,

$$\Delta_{e'g'} = [\omega_L-(\omega_{e'}-\omega_{g'})] \ , \tag{19}$$

and Ω_{eg} is half the Rabi frequency of the interaction of the field with atomic transition $|g\rangle$ to $|e\rangle$,

$$\Omega_{eg} = g_{eg}^{\lambda_L}\langle a_L(0)\rangle = g_{eg}^{\lambda_L *}\langle a_L^\dagger(0)\rangle \ , \tag{20}$$

where the Rabi frequency has been chosen as real (see Appendix A). A consequence of this choice of real Rabi frequency is that the generalized decay rates of Eq. (16) are also real (Appendix B).

The subset of atomic operator equations defined by Eqs. (18) is sufficient to describe the dynamic response of such atomic system observables as the populations. For the calculations presented in this work, the atoms are as-

sumed to be initially distributed equally among the ground states. This is represented by the conditions, at time equal to zero, as

$$\sum_g \langle \chi_{gg} \rangle = 1 \ , \tag{21a}$$

$$\langle \chi_{gg} \rangle = \langle \chi_{g'g'} \rangle \ . \tag{21b}$$

The general equations, Eqs. (18), are now applied to the problem of determining the time evolution of the population of the hyperfine states associated with the sodium D_2 transition. These states are illustrated in Fig. 1 together with a number label for each substate. As well as the initial conditions of Eqs. (21), it is also assumed that single-mode, coherent π-excitation radiation is tuned near to resonance with the $3^2S_{1/2}(F'=2) \rightarrow 3^2P_{3/2}(F=3)$ transition and that the intensity of the light is such that power broadening does not induce transitions from the $F'=1$ ground state. If specific knowledge of the populations of the $F'=1$ ground states is not required, then equations of motion of a 17-state system must be derived; the $F=2$, $m_F=0$ state, $|15\rangle$, is not excited. It is found that to obtain state population probabilities, the only elements required to be calculated are the diagonal terms, the optical coherences formed by the driving field and the coherences between pairs of upper states of the same m_F value connected to a common ground state by the excitation process. We call these terms "vertical-state coherences." The equations needed to calculate these elements form a closed subset of all possible equations; in this case 59 out of a possible 289. Thus the numerical calculations are considerably simplified. This number can be further reduced to 34 by recognizing the symmetry about the $m_F=0$ substates and appropriately adjusting branching ratios. However, physical interpretations are more readily made from the larger system of equations and so the discussion will be confined to it.

Six equations representative of those derived for the complete description are given in Table I. These equations describe the evolution of the $m_F=-2$ substates.

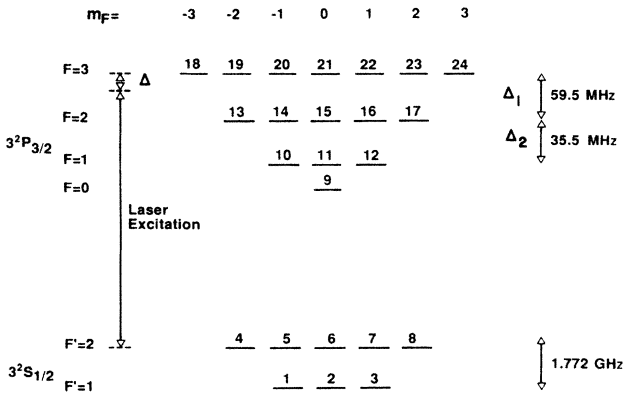

FIG. 1. D_2 line of sodium in hyperfine representation. The states are labeled for direct reference. Δ is the light detuning in rad s^{-1} from the $F'=2 \rightarrow F=3$ transition and Δ_1 (Δ_2) is the frequency splitting in rad s^{-1} of the $F=2$ ($F=1$) level from the $F=3$ ($F=2$) level.

TABLE I. Six representative equations from the closed subset of 59 equations describing the π excitation of the $3^2S_{1/2}(F'=2) \rightarrow 3^2P_{3/2}(F)$ transitions of the sodium D_2 line. These equations represent the time evolution of the $m_F=-2$ states. The first two equations are for the $F=3$ and $F=2$ excited states, respectively, while the third equation is for the $F'=2$ ground state. The optical coherences generated between these states are described in the fourth and fifth equations, while the last equation represents the evolution of the vertical-state coherence formed between the two excited states. Elements of the equations are placed in columns for reference in the text.

π-excitation equations	Frequency detuning and splitting	Driving terms	Einstein A coefficients	Generalized relaxation terms
$\langle \dot{\chi}_{19,19} \rangle$		$-i\Omega_{19,4}(\langle \chi_{19,4} \rangle - \langle \chi_{4,19} \rangle)$	$-\Gamma_{19}\langle \chi_{19,19} \rangle$	
$\langle \dot{\chi}_{13,13} \rangle$		$-i\Omega_{13,4}(\langle \chi_{13,4} \rangle - \langle \chi_{4,13} \rangle)$	$-\Gamma_{13}\langle \chi_{13,13} \rangle$	
$\langle \dot{\chi}_{44} \rangle$		$-i\Omega_{13,4}(\langle \chi_{4,13} \rangle - \langle \chi_{13,4} \rangle)$ $-i\Omega_{19,4}(\langle \chi_{4,19} \rangle - \langle \chi_{19,4} \rangle)$	$+\Gamma_{10,4}\langle \chi_{10,10} \rangle$ $+\Gamma_{13,4}\langle \chi_{13,13} \rangle$ $+\Gamma_{14,4}\langle \chi_{14,14} \rangle$ $+\Gamma_{19,4}\langle \chi_{19,19} \rangle$ $+\Gamma_{20,4}\langle \chi_{20,20} \rangle$	$+\Gamma_{19,13,4}(\langle \chi_{19,13} \rangle + \langle \chi_{13,19} \rangle)$ $+\Gamma_{14,10,4}(\langle \chi_{14,10} \rangle + \langle \chi_{10,14} \rangle)$ $+\Gamma_{20,10,4}(\langle \chi_{20,10} \rangle + \langle \chi_{10,20} \rangle)$ $+\Gamma_{20,14,4}(\langle \chi_{20,14} \rangle + \langle \chi_{14,20} \rangle)$
$\langle \dot{\chi}_{19,4} \rangle$	$-i\Delta\langle \chi_{19,4} \rangle$	$-i\Omega_{19,4}(\langle \chi_{19,19} \rangle - \langle \chi_{44} \rangle)$	$-i\Omega_{13,4}\langle \chi_{19,13} \rangle$	$-\Gamma_{19}\langle \chi_{19,4} \rangle/2$	
$\langle \dot{\chi}_{13,4} \rangle$	$-i(\Delta+\Delta_1)\langle \chi_{13,4} \rangle$	$-i\Omega_{13,4}(\langle \chi_{13,13} \rangle - \langle \chi_{44} \rangle)$	$-i\Omega_{19,4}\langle \chi_{13,19} \rangle$	$-\Gamma_{13}\langle \chi_{13,4} \rangle/2$	
$\langle \dot{\chi}_{19,13} \rangle$	$i\Delta_1\langle \chi_{19,13} \rangle$	$-i\Omega_{13,4}\langle \chi_{19,4} \rangle$ $+i\Omega_{19,4}\langle \chi_{4,13} \rangle$		$-(\Gamma_{19}+\Gamma_{13})\langle \chi_{19,13} \rangle/2$

The equations are arranged in columns for discussion purposes. The oscillatory term in column 1 for the optical coherences arises from the detuning of the light, whereas the corresponding term in the equation for the vertical-state coherence is the origin of quantum beats. Columns 2 and 3 contain the terms which describe the coupling of the atomic system with the driving field. The spontaneous-emission relaxation terms are found in column 4. In semiclassical theories, these terms are added to the density-matrix-element equations phenomenologically. The generalized relaxation terms are listed in column 5 in the equation for the population of the ground state $|4\rangle$.

A few notes of clarification of the derivation of the equations represented by Table I follow. The total relaxation rate out of each excited state will be identical since their lifetimes are the same. For example, Γ_{19} and Γ_{13} will have the same value. During the derivation, terms consisting of sums over all connected ground states of generalized relaxation terms from a specific pair of excited states arise in the equations for excited-state populations, vertical-state coherences, and optical coherences. For example, the term $\Gamma_{19,13,4}+\Gamma_{19,13,5}$ appears in the equation for $\langle\chi_{19,19}\rangle$ as the coefficient of the vertical-state coherence term $\langle\chi_{13,19}\rangle$. All such terms are zero. The specifically mentioned sum is used as an example. From Eq. (16a) and Appendix B we have

$$\Gamma_{19,13,4}+\Gamma_{19,13,5}=2\pi(g^{0*}_{19,4}g^{0}_{13,4}+g^{-*}_{19,5}g^{-}_{13,5}) , \tag{22}$$

where the superscripts 0 and $-$ represent π and σ^- modes, respectively. From Eqs. (A2) and (A8) of Appendix A, the product of the coupling constants is directly proportional to the product of the corresponding C factors which are given in Table II. Substitution of the appropriate C factors into Eq. (22) yields zero for the sum. Similarly, all other such summations are zero. As a result, the generalized decay constants only appear in the equations for the ground-state populations.

B. Semiclassical theory

Adoption of a classical field model and the use of the density operator to describe the atomic ensemble lead to the operator equation of motion,[9]

$$\dot{\rho}=-\frac{i}{\hbar}[H,\rho]+(\text{relaxation terms}) , \tag{23}$$

where the Hamiltonian consists of the free-atom part plus the quantum-mechanical interaction of the field with the atom. As mentioned above, the relaxation terms are added phenomenologically. The density-matrix elements and the atomic-operator elements of Sec. II A are related at time t by

$$\rho_{ji}(t)=\langle\sigma_{ij}(t)\rangle , \tag{24}$$

where $\langle\ \rangle$ represents the expectation value.

With reference to Table I, the equations of motion for the complete semiclassical theory can be obtained by ignoring the terms of column 5, the generalized relaxation terms. Thus, symbolically, the equations for the excited-state populations, optical coherences, and vertical-state coherences in the QED and semiclassical descriptions are identical. Both models predict the same rate of decay for

TABLE II. Values of Rabi frequency per unit square-root intensity [MHz/(mW/mm^2)$^{1/2}$] for each possible transition between hyperfine substates of the sodium D_2 line.

		$3^2S_{1/2}(F'=1)\rightarrow 3^2P_{3/2}(F)$				
				m_F		
Δm_F	F	-2	-1	0	1	2
1	0		16.1114			
1	1		18.0131	18.0131		
1	2		8.0557	13.9529	19.7324	
0	0			16.1114		
0	1		-18.0131	0	18.0131	
0	2		-13.9529	-16.1114	-13.9529	
-1	0				-16.1114	
-1	1			18.0131	18.0131	
-1	2		-19.7324	-13.9529	-8.0557	

		$3^2S_{1/2}(F'=2)\rightarrow 3^2P_{3/2}(F)$				
				m_F		
Δm_F	F	-2	-1	0	1	2
1	1	8.8246	6.2399	3.6026		
1	2	11.3925	13.9529	13.9529	11.3925	
1	3	7.2052	12.4799	17.6492	22.7850	27.9058
0	1		6.2399	7.2053	6.2399	
0	2	-16.1114	-8.0557	0	8.0557	16.1114
0	3	-16.1114	-20.3795	-21.6157	-20.3795	-16.1114
-1	1			-3.6026	-6.2399	-8.8246
-1	2		11.3925	13.9529	13.9529	11.3925
-1	3	-27.9058	-22.7850	-17.6492	-12.4799	-7.2052

the excited states in a situation where the atoms are first prepared by a driving field and then allowed to evolve freely. However, in the presence of a field, comparisons cannot be made by inspection of the equations. This work concentrates on the evaluation of the population terms. These terms are important for calculating such experimental observables as fluorescence, line polarization, and the intensity of superelastically scattered electrons. Where evaluation of the susceptibility of the atomic medium is required for experiments in which the transmitted light is detected, the optical coherences are the relevant terms. Application of the theory to the calculation of the time evolution of the optical coherences (coherent optical transients) of the D lines is reserved for a subsequent paper.

McClelland and Kelley[10] used a simplified semiclassical model. They ignored the contributions of the vertical-state coherences and so their model also did not include the terms in column 3 and the sixth equation of Table I. It should be noted that if each ground state could only be driven by radiation to a single excited state, then the generalized relaxation terms and the vertical-state coherences would not arise. Thus semiclassical and quantum-electrodynamical derivations would yield identical equations. This equivalence has been reported for two-level and three-level atomic systems.[16,17] Describing the sodium D_2 transition under the excitation conditions discussed in Sec. II A using the McClelland-Kelley model requires 41 equations, while 59 equations, the same number as for the QED model, are needed for the complete semiclassical description.

C. High-intensity state transformation

When the intensity of the injected light is high enough that power broadening mixes the excited-state hyperfine levels sufficiently so that they can be considered as degenerate, then Pegg and MacGillivray[14] have shown that it is possible to transform to a new basis for state description that simplifies the atom-light interaction model. In this section, we extend the earlier work to include relaxation terms.

We consider an atomic transition which has a manifold of lower states. Each lower state $|g\rangle$ can be excited to a number of upper states $|e\rangle$ where the number will vary depending on the total angular momentum of the upper level, selection rules, and the polarization of the exciting radiation. An upper state in the transformed basis is formed by the superposition of states $|e\rangle$ given by

$$|a\rangle=\sum_e \Omega_{eg}\beta_{ag}^{-1}|e\rangle\ , \tag{25}$$

where

$$\beta_{ag}^2=\sum_e \Omega_{eg}^2\ . \tag{26}$$

The half Rabi frequency Ω_{eg} is again taken as real. If there are n excited states involved in the particular transition, then another $n-1$ superposition states are formed which are orthogonal to $|g\rangle$ and $|a\rangle$.

Since now each ground state $|g\rangle$ can be driven only to a single excited state, a semiclassical model may be used as observed above. The total Hamiltonian can be written in the rotating reference-frame form[22] as the sum of terms H_g describing the excitation of each ground state to its excited-state manifold. Each term has the form

$$H_g=-\sigma_{gg}\Delta_{eg}+\sum_e \Omega_{eg}(\sigma_{ge}+\sigma_{eg})\ , \tag{27}$$

where Δ_{eg} is the detuning defined in Eq. (19).

It follows that the on-resonance Rabi frequency for the two-state system $|g\rangle$ and $|a\rangle$ is given by[14]

$$\langle g|H_g|a\rangle=\beta_{ag}\ . \tag{28}$$

The lifetimes of the excited states will be unchanged by the basis transformation. To include relaxation in this model, the branching ratios of the various relaxation channels from state $|a\rangle$ must be determined. It follows from the definition of oscillator strengths[23] that the rate of relaxation from state $|a\rangle$ to a lower state $|g'\rangle, \Gamma_{ag'}$, will be proportional to the square of the modulus of the matrix element $\langle g'|H_{g'}|a\rangle$. Using Eqs. (27) and (25) for the Hamiltonian and the transformed state yields

$$\langle g'|H_{g'}|a\rangle=\sum_e \Omega_{eg'}\Omega_{eg}\beta_{ag}^{-1}\ . \tag{29}$$

Representing the right-hand side of Eq. (29) by $\beta_{ag'}$, the relaxation rate $\Gamma_{ag'}$ is given by

$$\Gamma_{ag'}=\frac{\beta_{ag'}^2\Gamma_a}{\sum_{g'}\beta_{ag'}^2}\ , \tag{30}$$

where Γ_a is the total relaxation rate out of state $|a\rangle$ and is the inverse of the state lifetime.

Applied to the sodium D_2 transition the transformed basis representation appears as presented in Fig. 2. The radiation tuning conditions and polarization are the same as used previously, that is, the $F'=2$ ground state is excited by π excitation. The radiation power cannot be so high as to cause significant excitation from the $F'=1$ ground state.

Using Eqs. (29) and (30) and Table II, the branching ratios for relaxation from the excited states in the scheme of Fig. 2 can be calculated and these are given in Table

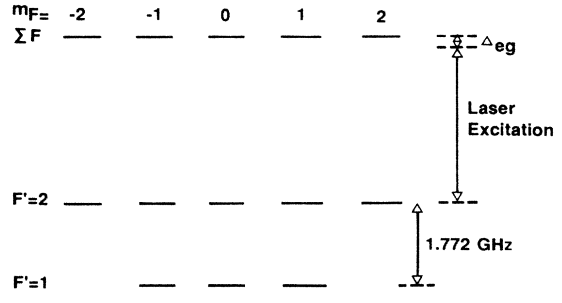

FIG. 2. States of the sodium D_2 line participating in the optical-pumping processes in the high-intensity limit. The excited states have been transformed to a new basis set.

TABLE III. Branching ratios from the π excitation–transformed excited states to the ground states for the sodium D_2 transition expressed as fractions of the total relaxation rate from an excited state.

				$\sum_{m_F} F$		
F'	Δm_F	-2	-1	0	1	2
2	-1		$\frac{1}{12}$	$\frac{1}{8}$	$\frac{1}{8}$	$\frac{1}{12}$
2	0	$\frac{2}{3}$	$\frac{2}{3}$	$\frac{2}{3}$	$\frac{2}{3}$	$\frac{2}{3}$
2	1	$\frac{1}{12}$	$\frac{1}{8}$	$\frac{1}{8}$	$\frac{1}{12}$	
1	-1			$\frac{1}{24}$	$\frac{1}{8}$	$\frac{1}{4}$
1	0		0	0	0	
1	1	$\frac{1}{4}$	$\frac{1}{8}$	$\frac{1}{24}$		

III. The values are expressed as fractions of the excited-state total relaxation rate Γ which, for the sodium D transitions, is 16 ns^{-1}. As is evident from Table III the excited state $m_F=1$ cannot relax to the ground state $F'=1$, $m_{F'}=1$. This is because, following the basis transformation, these two states are orthogonal. Similarly, the excited states $m_F=0$ and -1 are orthogonal to the lower states $F'=1$, $m_{F'}=0$ and -1, respectively. For the

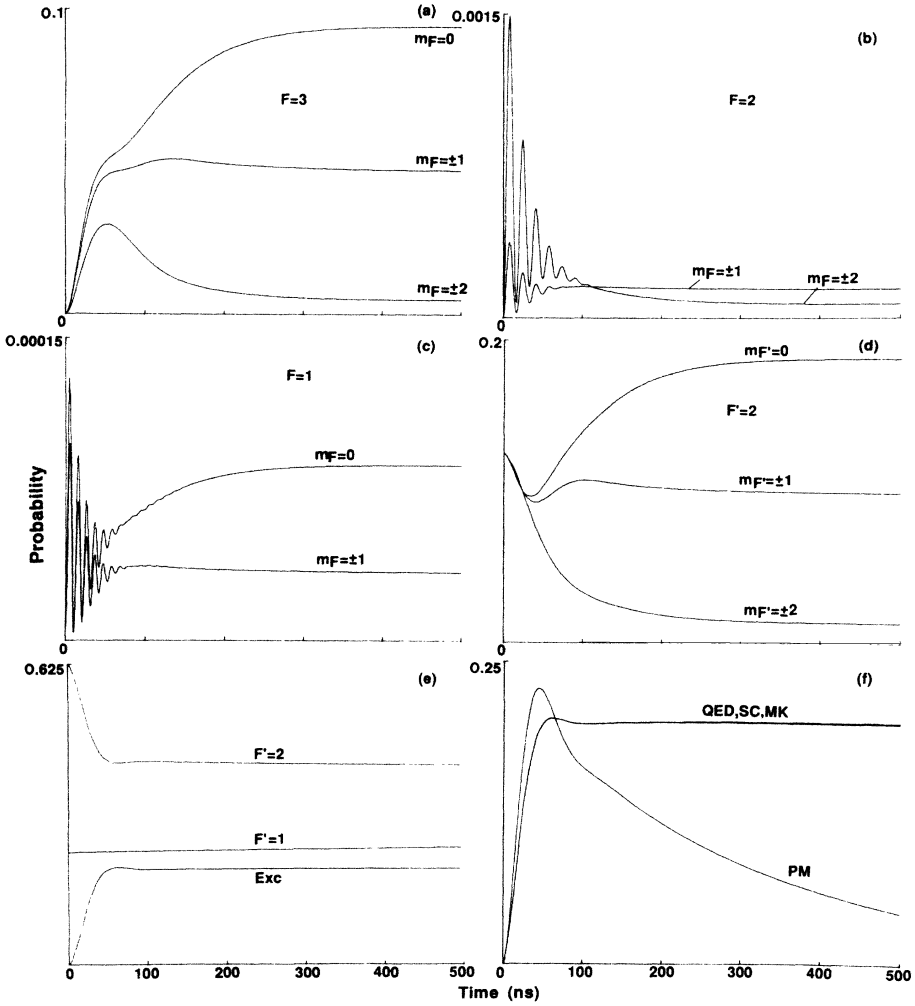

FIG. 3. Time evolution of hyperfine state and substate probabilities of the sodium D_2 line for 0.214 mW/mm^2 intensity light tuned to the $3^2S_{1/2}(F'=2)\rightarrow 3^2P_{3/2}(F=3)$ transition and inducing π excitation. (a) $F=3$ excited states, (b) $F=2$ excited states, (c) $F=1$ excited states, (d) $F'=2$ ground states, (e) $F'=2$ and $F'=1$ total probability and total excited-state probability, and (f) comparison of total excited-state probability for different models. QED, quantum electrodynamic; SC, semiclassical; MK, McClelland-Kelley; PM, Pegg-MacGillivray.

Pegg-MacGillivray model, 20 equations describe the sodium D_2 line excitation of Sec. II A.

III. CALCULATIONS AND COMMENTS

The equations to be solved form sets of coupled, first-order, linear, homogeneous differential equations with constant coefficients, which may be written as

$$\dot{\mathbf{y}} = \underline{A}\mathbf{y} , \tag{31}$$

where the vector $\mathbf{y}$ consists of the operator elements in arbitrary order. The elements of matrix $\underline{A}$ consist of combinations of Rabi frequencies, relaxation rates, energy-level frequency splittings, and incident-radiation–atomic-transition frequency detunings. The eigenvalues λ_i and the associated matrix of eigenvectors $\underline{X}$ of $\underline{A}$ are obtained by diagonalizing $\underline{A}$ using subroutines from EISPAC.[24] The solutions of the elements of $\mathbf{y}$ are then given by

$$y_j(t) = \sum_i \alpha_i X_{ij} e^{\lambda_i t} , \tag{32}$$

where $\boldsymbol{\alpha}$ relates to the initial conditions via

$$\underline{X}\boldsymbol{\alpha} = \mathbf{y}(0) . \tag{33}$$

For all examples calculated here, the initial conditions were such that the ground-state populations were set at 0.125 each.

Figure 3 presents calculations of the probabilities of finding atoms in various states for an input light intensity of 0.214 mW/mm^2 or, alternatively, a Rabi frequency of 10 MHz for the $3^2S_{1/2}(F'=2, m_{F'}=0) \rightarrow 3^2P_{3/2}(F=3, m_F=0)$ transition which is the strongest transition in the manifold. π excitation is assumed. In Fig. 3(a) the $3^2P_{3/2}$ $(F=3)$ substate probabilities are plotted as a function of time. The curves illustrate the optical pumping towards the center substates; that is, the substates with small m_F values. The $F=2$ and $F=1$ excited-level substates are shown in Figs. 3(b) and 3(c), respectively. There is very little excitation of these levels since the weak input light is tuned to the $F'=2 \rightarrow F=3$ transition. The substate populations for these levels exhibit nutational oscillations at their respective frequency splittings from the $F=3$ level which is the detuned frequency of the $F'=2 \rightarrow F=2,1$ transitions from the frequency of the light. The optical pumping to the center substates in the $F=3$ level is mirrored in the $F'=2$ ground substates as shown in Fig. 3(d). In Fig 3(e), the total of the excited states' probability is plotted along with the total $F'=2$ and $F'=1$ ground states' populations. As was noted with the rate-equation calculations,[6,7] the total excited-level population reaches a steady-state value at a time well before each individual substate reaches a constant value. On the scale of Fig. 3(e), it is apparent that losses into the $F'=1$ ground state are negligible. This follows from the fact that the $F=3$ level cannot decay to this level and the overlapping of the $F'=2 \rightarrow F=3,2,1$ transitions is minimal at these light intensities. Finally, a comparison of the various models discussed in Sec. II is given in Fig. 3(f), where the total excited-state population is plotted. No difference can be discerned between the QED, semiclassical, and McClelland-Kelley models. The Pegg-MacGillivray description shows decay out of the $F'=2 \rightarrow F=3,2,1$ system because the transformed excited state can relax to the $F'=1$ ground state. Clearly, the Pegg-MacGillivray model is not applicable at this laser intensity since the condition of degeneracy of the excited states is not satisfied because the hyperfine-state frequency splittings are greater than the Rabi frequencies.

The calculations are repeated in Fig. 4 for a laser intensity of 85.6 mW/mm^2 $[3^2S_{1/2}(F'=2, m_{F'}=0) \rightarrow 3^2P_{3/2}(F=3, m_F=0)$ Rabi frequency of 200 MHz], this being an easily obtainable intensity from a ring dye laser. At this intensity, the pumping to the $F'=1$ ground state dominates the other optical processes since the transitions in the manifold are now well mixed by power broadening. Eventually, all of the atoms will be found in the $F'=1$ ground-state level [Fig. 4(e)]. The excited states, in particular, exhibit complicated nutational oscillations reflecting the contributions of the different Rabi frequencies for the individual hyperfine transitions [Figs. 4(a)–4(c)]. It is interesting to note in Fig. 4(e) that, even after the Rabi oscillations have decayed away, it is more probable to find an atom in an excited state than in the $F'=2$ ground state. However, there is no inversion in any of the two-state m_F transitions. The other models are compared to the QED description in Fig. 4(f) using the total excited-state probability. Again, the semiclassical calculation yields no discernible difference. The fact that the McClelland-Kelley and the Pegg-MacGillivray plots agree closely is due to a quite fortuitous choice of input intensity. For all but a small region of intensities these theories exhibit considerable differences in their calculations as shown in Fig. 5(b).

In Fig. 5(a), the probability of finding the atom in the excited-state manifold and in each of the two ground-state levels is plotted as a function of input light intensity expressed as the Rabi frequency of the $3^2S_{1/2}(F'=2, m_{F'}=0) \rightarrow 3^2P_{3/2}(F=3, m_F=0)$ transition. Each probability has been time averaged over 1 μs, an estimate of the time an atom would take to traverse a laser beam of 1 mm diameter perpendicular to its direction of travel. The probability of an atom being in an excited state is a maximum at a relatively low input intensity (1.15 mW/mm^2). This is somewhat lower than the 10 mW/mm^2 predicted as the intensity of reaching this maximum probability by the rate-equation approach.[6] The predictions of Fig. 5(a) indicate that in performing experiments (such as superelastic electron scattering) which are dependent on having a significant fraction of sodium atoms prepared in the $3^2P_{3/2}$ level in an highly collimated beam, input light of high intensity is not required and is possibly detrimental. The calculations of the various models for the time-averaged probability as a function of light intensity are shown in Fig. 5(b). At low intensities the QED, semiclassical, and McClelland-Kelley descriptions converge while the QED calculation asymptotically approaches the Pegg-MacGillivray values at high intensities.

Because the $3^2P_{3/2}$ manifold of states is transformed to

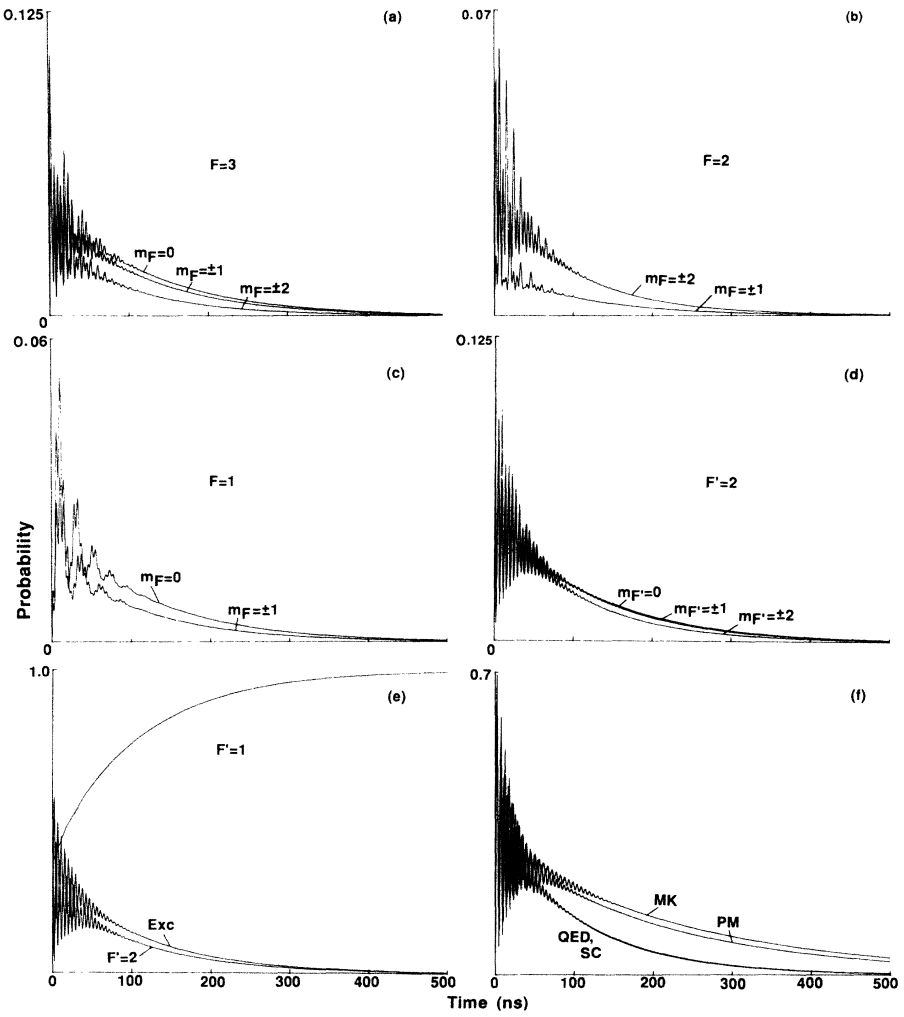

FIG. 4. Same as for Fig. 3 but with an intensity of 85.6 mW/mm^2.

a single level in the Pegg-MacGillivray model, the equations derived from this description do not contain any vertical coherence terms nor generalized relaxation terms. However, this model is exact at the high-intensity limit where the energy-level splittings in the excited-state manifold are negligible compared with the Rabi frequencies. That the QED probability converges to that of the Pegg-MacGillivray model at high intensity would seem to validate such approximations in the purely quantum theory as the generalized relaxation terms being real. Figure 5(b) shows that the Pegg-MacGillivray model provides reasonably accurate calculations even at moderate intensities. This theory has the advantage of being the simplest description in terms of numbers of equations and hence is the fastest to calculate. The semiclassical and the QED curves diverge at a Rabi frequency at around 300 MHz, indicating that the generalized relaxation terms play a significant role above this intensity.

The QED model excited-state, time-averaged probability was also calculated for a Doppler-broadened atomic medium. The atomic velocity profile was assumed to be Gaussian and so the solutions to the equations were integrated over the Doppler detuning after being weighted by

$$\frac{1}{\Delta_0\sqrt{\pi}}\exp[-(\Delta/\Delta_0)^2] .$$

The excited-level probability as a function of light intensity for Δ_0 equal to $4\pi\times10^{-8}$ rad s^{-1} is shown in Fig. 6. This value of Δ_0 represents a sodium atomic beam with a collimation rate of about 5:1. The probability of finding an atom in the medium in an excited state is greatly reduced from the homogeneously broadened case because of the velocity distribution. This curve also indicates that, for a poorly collimated atomic beam, the greater the light intensity the larger the fraction of $3^2P_{3/2}$-state atoms since those in the wings of the velocity profile have a higher probability of being excited.

Figure 7 shows the calculated, time-averaged probability of an atom being in the $3^2P_{3/2}$ level as a function of input radiation intensity when the input light is circularly polarized. σ^+ excitation is assumed. As for the π excitation, there are no discernible differences between the QED, semiclassical, and McClelland-Kelley models at

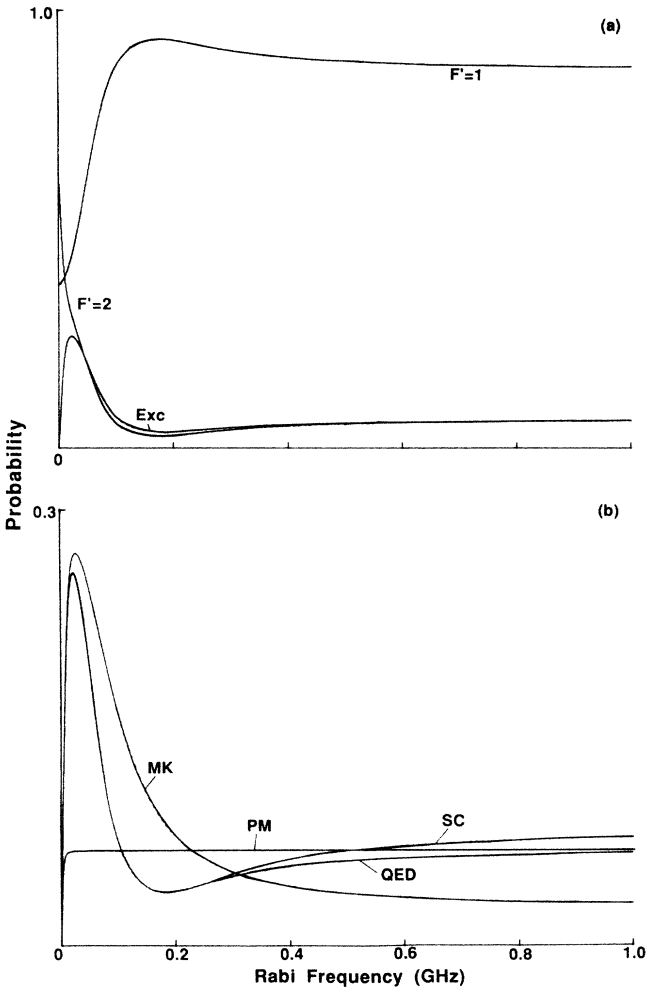

FIG. 5. (a) 1-μs time-average probabilities for the $F'=1$ and $F'=2$ ground states and total excited level as a function of intensity for π-excitation radiation. The intensity is expressed in terms of the Rabi frequency of the $3^2S_{1/2}(F'=2, m_{F'}=0) \rightarrow 3^2P_{3/2}(F=3, m_F=0)$ transition. Calculation is via the QED description. (b) Comparison of the 1 μs time-averaged total excited level as a function of laser intensity for the various models.

low intensity. At high intensity, the QED and semiclassical calculations converge to the Pegg-MacGillivray values. For σ^+ excitation, the atoms that remain in the influence of the light are pumped to the $F'=2, m_{F'}=2 \rightarrow F=3, m_F=3$ transition after several lifetimes. These atoms are then effectively in a pure two-state system and their evolution can be described in terms which do not include vertical coherences or generalized relaxation terms. These relaxation terms, which have characteristic times of the order of the atomic lifetime, thus do not play a significant role in the σ^+ excitation scheme. This is why the QED and semiclassical curves do not diverge in Fig. 7. On the other hand, the characteristic time of the vertical coherences is the period of the Rabi frequency and so the McClelland-Kelley model calculation differs significantly from the QED calculation above the weak intensity limit.

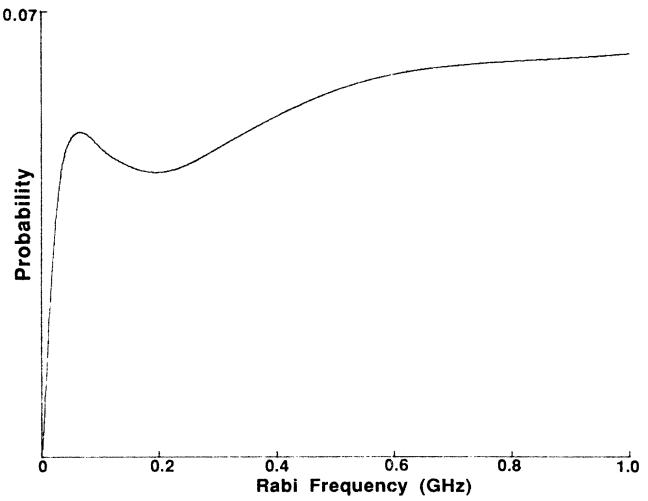

FIG. 6. QED model calculations for the Doppler integrated ($\Delta_0=4\pi\times10^8$ rad s^{-1}) total excited-level probability as a function of the intensity of π-excitation radiation.

IV. CONCLUSION

The main conclusion of this work is that it is feasible to carry out numerical calculations of complete QED operator equations which describe the interaction of light with an atomic transition of quite complicated energy-level structure without neglecting important terms. All relevant state coherences and generalized relaxation terms can be included. The generalized relaxation terms as well as the usual Einstein A coefficient terms arise naturally in the QED derivation as opposed to the semiclas-

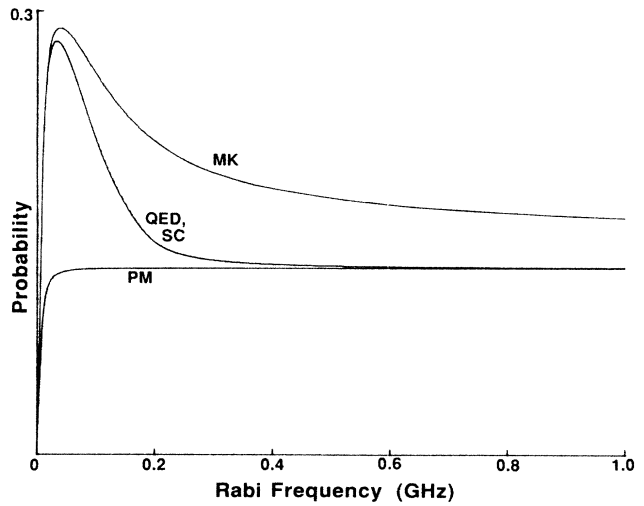

FIG. 7. Comparison of the 1 μs time-averaged total excited-state probability calculated by the various models as a function of the intensity for σ^+-excitation radiation. The intensity is expressed as the Rabi frequency of the $3^2S_{1/2}(F'=2, m_{F'}=2) \rightarrow 3^2P_{3/2}(F=3, m_F=3)$ transition.

sical, density-matrix model, where all relaxation terms are added in an *ad hoc* manner and the second-order terms have never been included. However, a semiclassical model which neglects only the generalized relaxation terms yields no appreciable saving of computing time. Reduction of the number of system equations by further approximation can produce unphysical results. For example, in the model of McClelland and Kelley, in which the vertical-state coherences of the hyperfine levels of the $3^2P_{3/2}$ level of the sodium D_2 transition are omitted, the probability of finding an atom in the ground state $3^3S_{1/2}(F'=2)$ goes, transiently, negative for quite moderate, π-polarization, light intensities (~ 80 mW/mm^2). On the other hand, in the weak-intensity limit, the McClelland-Kelley and QED models produce similar results.

For excitation schemes in which each ground state can be excited to only one upper state, the semiclassical and QED models yield identical equations. This is not the case for the transition studied in this work, the $3^2S_{1/2}(F'=2)\rightarrow 3^2P_{3/2}(F=3,2,1)$ scheme of sodium. However, at laser intensities high enough that the excited-state splittings can be neglected compared with the Rabi frequencies, the upper level can be transformed to a new basis in which each ground state can be excited to, at most, one state. This allows for a simplified, semiclassical description with significant computational savings. In fact, this model yields results that compare well with calculations from the QED model at even moderate intensities. Finally, when a highly collimated beam of atomic sodium is irradiated by a narrow-band, monochromatic laser tuned to the above transition, the probability of finding an atom in the $3^2P_{3/2}$ level does not continuously increase with light intensity but rather has its maximum value at quite a low intensity, the value depending on the form of excitation.

ACKNOWLEDGMENTS

The authors acknowledge useful discussions with Dr. P. L. Knight and Professor D. T. Pegg. The work was funded principally by the Australian Research Grants Scheme. One of us (P.M.F.) was supported by the Australian Government Postgraduate Research Fund.

APPENDIX A

The Rabi frequency is defined as

$$\Omega=-\mathbf{E}\cdot\mathbf{D}/\hbar\ , \tag{A1}$$

where $\mathbf{E}$ is the electric field and $\mathbf{D}$ is the induced dipole operator. Equivalently, the Rabi frequency is given, in terms of the electric field operators, as

$$\Omega_\lambda=2g_\lambda\langle a_\lambda(0)\rangle=2g_\lambda^*\langle a_\lambda^\dagger(0)\rangle\ , \tag{A2}$$

where the Rabi frequency has been taken as real. That Ω can be considered as a real quantity follows from the freedom to choose the phase of the field and the phases of the states connected with the induced dipole.[25]

Considering only the field amplitudes $\mathbf{E}$ can be written in terms of the spherical unit vectors $\hat{\mathbf{e}}_q$ as[23]

$$\mathbf{E}=\sum_{q=-1}^{1}(-1)^q E_q\hat{\mathbf{e}}_{-q}\ , \tag{A3}$$

where

$$\hat{\mathbf{e}}_{\pm1}=\mp\frac{1}{\sqrt{2}}(\mathbf{i}\mp i\mathbf{j})\ , \tag{A4a}$$

$$\hat{\mathbf{e}}_0=\mathbf{k}\ . \tag{A4b}$$

If $\mathbf{D}$ is written in terms of the same basis, then we have

$$\mathbf{E}\cdot\mathbf{D}=-E_{-1}D_1-E_1D_{-1}+E_0D_0\ . \tag{A5}$$

For circularly polarized light, the field amplitudes are chosen such that

$$E_{\pm1}=\mp E_C\ . \tag{A6}$$

Then, taking the usual definitions for $\sigma^\pm$ and π transitions, the on-resonance Rabi frequencies are

$$\Omega_\pi=-\frac{E_0}{\hbar}\langle JM\mid D_0\mid J'M\rangle\ , \tag{A7a}$$

$$\Omega_{\sigma^+}=\frac{E_c}{\hbar}\langle JM+1\mid D_1\mid J'M\rangle\ , \tag{A7b}$$

$$\Omega_{\sigma^-}=-\frac{E_c}{\hbar}\langle JM-1\mid D_{-1}\mid J'M\rangle\ , \tag{A7c}$$

where the primed state is the lower state.

The dipole operator D_q is an irreducible tensor operator of rank 1. The matrix elements of Eqs. (A7) can be evaluated using the Wigner-Eckart theorem to remove the M dependence and then the reduction theorem for composite systems.[26] Alternatively, the equivalent "T" matrix formalism and reduction theorems of Condon and Shortley[27] can be employed. The remaining reduced matrix elements, for example $(L\|D\|L')$, can be evaluated in terms of the Einstein A coefficient of the transition.[28]

Rabi frequencies $\nu(F',M_{F'},F,M_F,q)$ are evaluated for transitions between the hyperfine states of the sodium D_2 line,

$$\nu(F',M_{F'},F,M_F,q)=C(F',M_{F'},F,M_F,q)I^{1/2}\ \text{(MHz)}\ , \tag{A8}$$

where

$$C(F',M_{F'},F,M_F,q)=(-1)^{F+F'+J+J'+I+L+S-M_F+1}\times 868\left[\frac{3\epsilon_0\hbar\lambda^3\Gamma_{LL'}}{8\pi^2}\right]^{1/2}$$
$$\times[(2F+1)(2F'+1)(2J+1)(2J'+1)(2L+1)]^{1/2}$$
$$\times\begin{Bmatrix}F & 1 & F'\\ -M_F & q & M_{F'}\end{Bmatrix}\begin{Bmatrix}J & F & I\\ J' & L' & 1\end{Bmatrix}\begin{Bmatrix}L & J & S\\ J' & L' & 1\end{Bmatrix}\Big/h\ \ [\text{MHz}/(\text{mW}/\text{mm}^2)^{1/2}]\ . \tag{A9}$$

From Eq. (A7b), Eq. (A9) is multiplied by a further negative one when q is equal to 1. The values of the C factor for the D_2 transition of sodium are given in Table II. It should be noted that the values in this table are numerically the same as those given in Table I of Pegg and MacGillivray[14] but the signs of the $\Delta m_F = -1$ terms are the opposite. In calculating the values in the previous work, the relationship (A1) was defined as a positive equation and the C factor was expressed in terms of the reduced matrix in J rather than that in L as here. As well, the sign change from Eq. (A7b) was not included. The signs arising from Eqs. (A7) are implicit in the Condon-Shortley formalism[27] and all signs were checked using their expressions.

APPENDIX B

The half Rabi frequency term as defined by Eq. (20) can be written as

$$\Omega_{eg} = | g_{eg}^{\lambda_L} | e^{i\alpha} | \langle a_L(0) \rangle | e^{i\beta} . \tag{B1}$$

Since the Rabi frequency has been chosen as real, then

$$\alpha + \beta = n\pi \quad (n \equiv \text{integer}) . \tag{B2}$$

Similarly,

$$\Omega_{e'g} = | g_{e'g}^{\lambda_L} | e^{i\gamma} | \langle a_L(0) \rangle | e^{i\beta} , \tag{B3}$$

where

$$\gamma + \beta = m\pi \quad (m \equiv \text{integer}) . \tag{B4}$$

The generalized decay terms connecting two excited states to one ground state contain products of the form

$$g_{eg}^{\lambda} g_{e'g}^{\lambda *} = | g_{eg}^{\lambda} | | g_{e'g}^{\lambda} | e^{i(\alpha - \gamma)} . \tag{B5}$$

From Eqs. (B2) and (B4),

$$\alpha - \gamma = (n - m)\pi . \tag{B6}$$

If n and m are either both odd or both even, the product term will be real and positive. If one of n and m is even and the other odd, then the product will be real and negative.

[1] R. Schieder and H. Walther, Z. Phys. **270**, 55 (1974).
[2] J. A. Abate, Opt. Commun. **10**, 269 (1974).
[3] R. E. Grove, F. Y. Wu, and S. Ezekiel, Phys. Rev. A **15**, 227 (1977).
[4] See, for example, S. Haroche, in *High-Resolution Laser Spectroscopy*, edited by K. Shimoda (Springer-Verlag, Berlin, 1976).
[5] R. Walkup, A. L. Migdall, and D. E. Pritchard, Phys. Rev. A **25**, 3114 (1982).
[6] I. V. Hertel and W. Stoll, J. Appl. Phys. **47**, 214 (1976).
[7] I. V. Hertel and W. Stoll, Adv. At. Mol. Phys. **13**, 113 (1977).
[8] V. I. Balykin, Opt. Commun. **33**, 31 (1980).
[9] See, for example, L. Allen and J. H. Eberly, *Optical Resonance and Two-Level Atoms* (Wiley, New York, 1975).
[10] J. J. McClelland and M. H. Kelley, Phys. Rev. A **31**, 3704 (1985).
[11] J. J. McClelland, M. H. Kelley, and R. J. Celotta, Phys. Rev. Lett. **55**, 688 (1985).
[12] J. J. McClelland, M. H. Kelley, and R. J. Celotta, Phys. Rev. Lett. **56**, 1362 (1986).
[13] J. J. McClelland, M. H. Kelley, and R. J. Celotta, J. Phys. B **20**, L385 (1987).
[14] D. T. Pegg and W. R. MacGillivray, Opt. Commun. **59**, 113 (1986).
[15] J. R. Ackerhalt, P. L. Knight, and J. H. Eberly, Phys. Rev. Lett. **30**, 456 (1973).
[16] J. R. Ackerhalt and J. H. Eberly, Phys. Rev. D **10**, 3350 (1974).
[17] R. M. Whitley and C. R. Stroud, Phys. Rev. A **14**, 1498 (1976).
[18] P. W. Milonni, Phys. Rep. **25**, 1 (1976).
[19] P. L. Knight, Opt. Commun. **32**, 261 (1980).
[20] D. A. Cardimona, M. G. Raymer, and C. R. Stroud, J. Phys. B **15**, 55 (1982).
[21] D. A. Cardimona and C. R. Stroud, Phys. Rev. A **27**, 2456 (1983).
[22] D. T. Pegg, in *Laser Physics*, edited by D. F. Walls and J. D. Harvey (Academic, Sydney, 1980).
[23] See, for example, A. Corney, *Atomic and Laser Spectroscopy* (Clarendon, Oxford, 1977).
[24] B. T. Smith, J. M. Boyle, J. J. Dongarra, B. S. Garbow, Y. Ikebe, V. C. Klema, and C. B. Moler, *Matrix Eigensystem Routines—EISPACK Guide* (Springer-Verlag, Berlin, 1976).
[25] M. Ducloy, Phys. Rev. A **8**, 1844 (1973).
[26] A. Messiah, *Quantum Mechanics* (North-Holland, Amsterdam, 1962).
[27] E. U. Condon and G. H. Shortley, *The Theory of Atomic Spectra* (Cambridge University Press, Cambridge, 1935).
[28] I. I. Sobelman, *Atomic Spectra and Radiative Transitions* (Springer-Verlag, Berlin, 1979).